Observations of stratospheric warmings and mesospheric coolings by the TIMED SABER instrument

D. E. Siskind and L. Coy
E.O. Hulburt Center for Space Research, Naval Research Laboratory, Washington, D. C., USA

P. Espy
Physical Sciences Division, British Antarctic Survey, Natural Environment Research Council, Cambridge, UK

Received 10 January 2005; revised 25 February 2005; accepted 8 April 2005; published 6 May 2005.

[1] We used temperature data from the Sounding of the Atmosphere with Broadband Emission Radiometry (SABER) on the the NASA TIMED satellite to quantify the connection between temperatures in the stratosphere and in the mesosphere and lower thermosphere. Specifically, we studied three winter periods where stratospheric temperatures were dynamically disturbed: February 2002, August, 2002, and February 2003. The SABER temperatures show a clear signature of mesospheric coolings in concert with stratospheric warmings. Mesospheric temperatures between 0.7 hPa and 0.01 hPa show a significant anticorrelation with stratospheric temperatures. For pressures <0.01 hPa, this anticorrelation breaks down, in disagreement with recent model results from a thermosphere-ionosphere-mesosphere general circulation model that suggest mesospheric coolings persist up to 110 km. Also, the lack of a clear correlation between stratospheric temperatures and those at 83–90 km suggests that measurements of the OH Meinel band temperatures at those altitudes may not be representative of the entire mesosphere. **Citation:** Siskind, D. E., L. Coy, and P. Espy (2005), Observations of stratospheric warmings and mesospheric coolings by the TIMED SABER instrument, *Geophys. Res. Lett.*, *32*, L09804, doi:10.1029/2005GL022399.

1. Introduction

[2] There is great interest in understanding the coupling mechanisms between the upper and lower atmosphere. Part of this stems from the suggestion [*Roble and Dickinson*, 1989; *Emmert et al.*, 2004] that significant cooling of the upper atmosphere should correlate with global warming of the troposphere. Also, it is now felt that meteorological disturbances at high altitudes can influence the dynamics of the lower atmosphere, and possibly effect the weather [*Baldwin and Dunkerton*, 2001]. One particularly dramatic meteorological disturbance which affects a wide range of altitudes in the high latitude winter middle atmosphere is sudden stratospheric warmings (SSWs). The largest SSWs are typically associated with dramatic wind reversals and temperature increases of up to 60K [*Labitzke*, 1981].

[3] It is also known that mesospheric coolings are associated with SSWs. *Liu and Roble* [2002] recently showed how the atmospheric response to an SSW could extend up through the mesosphere and thermosphere. Validating their model predictions is difficult because of lack of data. The most comprehensive relevant observations are the ground-based measurements of the rotational temperature of vibrationally excited OH in the Meinel band airglow (OH*). However, these measurements are confined to a narrow layer near 85–87 km altitude. There has been considerable uncertainty in connecting these data to stratospheric temperatures during SSWs.

[4] For example, using a 20 year long Meinel band data set from Svalbard (78N), *Sigernes et al.* [2003] state that while mesospheric coolings are associated with stratospheric warmings, they did not find the expected anticorrelation between airglow temperatures and stratospheric temperatures at 10 hPa. They also found no connection between the solar 10.7 cm flux (F107) and airglow temperature. This is in contrast to the results of *Hernandez* [2003], who found a strong correlation with F107. He also suggests a correlation between winter OH* temperatures over the South Pole and the size of the springtime Antarctic ozone hole [*Hernandez*, 2004]. *Cho et al.* [2004] report cooling of the upper mesosphere in concert with stratospheric warmings; however, the anticorrelation they show is between OH* temperatures and a meteorological analysis at 0.316 hPa (58 km), a level which is not stratospheric. When they correlate with an analysis at 3.16 hPa (40 km), no such general clear-cut relationship is seen (although an anticorrelation is seen for a short period of time in December 2001). Questions about the timing of stratospheric and mesospheric disturbances also remain. *Myrabo et al.* [1984] report a 1–2 day delay in the mesospheric response to a stratospheric event, and *Hernandez* [2004] suggests the mesosphere is a 1–2 month leading indicator of stratospheric warmings, while the model result of *Liu and Roble* [2002] indicates little, if any, phase lag or lead between the temperature anomalies in the mesosphere and stratosphere.

[5] In this paper, we use global temperature profiles from the Sounding of the Atmosphere using Broadband Emission Radiometry (SABER) experiment on the NASA Thermosphere Ionosphere Mesosphere Energetics and Dynamics (TIMED) satellite to quantify the relationship between stratospheric and mesospheric temperatures for a range of altitudes, latitudes and meteorological conditions. SABER data offer considerable advantages for the study of mesospheric cooling events. SABER provides high vertical resolution (<5 km) profile information from the tropopause into the lower thermosphere. SABER data can place the ground based measurements of OH* in a global context,

Report Documentation Page

Form Approved
OMB No. 0704-0188

1. REPORT DATE **APR 2005**	2. REPORT TYPE	3. DATES COVERED **00-00-2005 to 00-00-2005**

4. TITLE AND SUBTITLE **Observations of stratospheric warmings and mesospheric coolings by the TIMED SABER instrument**	5a. CONTRACT NUMBER
	5b. GRANT NUMBER
	5c. PROGRAM ELEMENT NUMBER
6. AUTHOR(S)	5d. PROJECT NUMBER
	5e. TASK NUMBER
	5f. WORK UNIT NUMBER
7. PERFORMING ORGANIZATION NAME(S) AND ADDRESS(ES) **Naval Research Laboratory,E. O. Hulburt Center for Space Research,Washington,DC,20375**	8. PERFORMING ORGANIZATION REPORT NUMBER
9. SPONSORING/MONITORING AGENCY NAME(S) AND ADDRESS(ES)	10. SPONSOR/MONITOR'S ACRONYM(S)
	11. SPONSOR/MONITOR'S REPORT NUMBER(S)

12. DISTRIBUTION/AVAILABILITY STATEMENT
Approved for public release; distribution unlimited

13. SUPPLEMENTARY NOTES

14. ABSTRACT

15. SUBJECT TERMS

16. SECURITY CLASSIFICATION OF:			17. LIMITATION OF ABSTRACT	18. NUMBER OF PAGES	19a. NAME OF RESPONSIBLE PERSON
a. REPORT **unclassified**	b. ABSTRACT **unclassified**	c. THIS PAGE **unclassified**	**Same as Report (SAR)**	**4**	

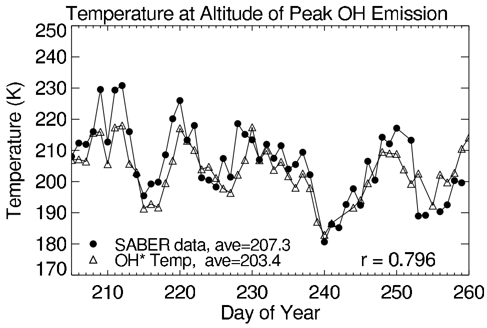

Figure 1. Comparison of SABER temperatures over Rothera, Antarctica with ground based measurements of the OH* airglow temperature. See text for details of averaging procedure. The overall mean temperatures are given in the lower left of the plot; the linear correlation between the two time series is given in the lower right of the plot.

quantify the height range for which mesospheric coolings occur, and allow a search for secondary thermospheric warmings as was predicted by *Liu and Roble* [2002].

2. Summary and Validation of SABER Data

[6] SABER is a 10 channel broadband, limb-viewing, infrared radiometer which has been measuring stratospheric and mesospheric temperatures since the launch of the TIMED satellite in December 2001. The temperature is obtained from the 15 μm radiation of CO_2. This emission is in LTE in the stratosphere and lower mesosphere and has been extensively discussed and validated by *Remsberg et al.* [2003]. In the middle to upper mesosphere and lower thermosphere (MLT), non-LTE conditions prevail; initial results from a non-LTE retrieval have been presented by *Mertens et al.* [2004]. Here we use exclusively retrievals with the non-LTE effects included (Version 1.04 in the SABER database).

[7] The TIMED satellite is in a nearly circular 625 km-altitude orbit with an inclination of 74°. The resulting latitudinal coverage extends over 135°, from 85° in one hemisphere to about 50° in the other. Every 60 days or so, the TIMED spacecraft executes a yaw maneuver which flips the dominant hemisphere covered by SABER. We focus on three wintertime periods when SABER measured up to near the pole: February, 2002 in the Northern Hemisphere (NH) (hereinafter Period 1), August, 2002 in the Southern Hemisphere (SH) (Period 2), and January and February, 2003 in the NH (Period 3). Period 2 is of particular interest because stratospheric warmings in the Austral winter are known to be weaker and less frequent than their NH counterparts and because the Antarctic ozone hole the following spring was unusually small [*Hernandez*, 2003].

[8] In order to validate our results at MLT altitudes, we compare our data against the OH* temperatures described by *Espy et al.* [2003]. These are shown in Figure 1 together with SABER temperatures within ±5° of latitude and ±15° of longitude of Rothera (68S). The SABER data are taken at the altitude of the peak 1.6 μm OH volume emission rate which is simultaneously retrieved along with the SABER temperatures. Figure 1 shows very good agreement in absolute magnitude and in variability between the ground based and satellite data. Since the temperature at lower altitudes has already been validated by *Remsberg et al.* [2003], we conclude that SABER temperatures are of high quality at least up to 85 km. In practice, useful retrievals are thought to extend up to 105 km; we will analyze these data with the understanding that validation is currently ongoing.

3. Analysis of Temperature Profiles

[9] Stratospheric meteorology differed for the three periods we studied. The SSW which occurred in Period 1 was an enhanced wave 1 event and is discussed in greater depth by *Remsberg et al.* [2003]. Period 2 was also dominated by wave 1 and is discussed in depth below. Period 3 was characterized by enhanced wave 2 [*McCormack et al.*, 2004]; for Period 3, the SABER observations begin at the peak of the warming and continue for 6 weeks thereafter. Thus, a consideration of these three events together allow us to make some general conclusions about the response of the MLT when the stratosphere is disturbed by planetary waves.

[10] Figure 2 plots time series of zonal mean SABER temperatures at 80°S for several altitudes during Period 2. A clear warming event of about 25K is seen at 10 hPa starting at Day 233 (Aug 21, 2002) and lasting several days. This is matched by a mesospheric cooling event seen in the 0.1 hPa temperatures. Other smaller fluctuations in the 10 hPa temperatures are seen which coincide with fluctuations of opposite sign at 0.1 hPa. Interestingly, while some of the fluctuations at 0.01 hPa match those at 0.1 hPa, for days 232–235, little if any change in temperature is seen at 0.01 hPa. This suggests that for this SSW, the mesospheric cooling did not extend to 80 km.

[11] Also apparent in Figure 2 are long-term monotonic temperature changes. These are likely related to the seasonal change in the radiative forcing, i.e. the increasing sunlight throughout the late winter. To isolate the short-term dynamical response of the atmosphere, we subtracted a linear fit from the temperature time series. We then calculated the cross-correlation coefficient, *r*, between the residual zonal mean temperature time series at every altitude from 100 hPa

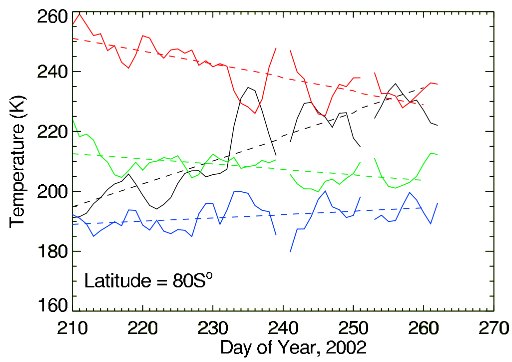

Figure 2. Time series of SABER zonal mean temperatures for SH winter 2002 for 4 pressures. Also shown is a linear fit to the temperature time series. This fit is subtracted from the time series before performing the correlation analysis summarized in Figure 3. The black curve is for 10.0 hPa, the red curve is for 0.1 hPa, the green curve is for 0.01 hPa and the blue curve is for 10^{-3} hPa.

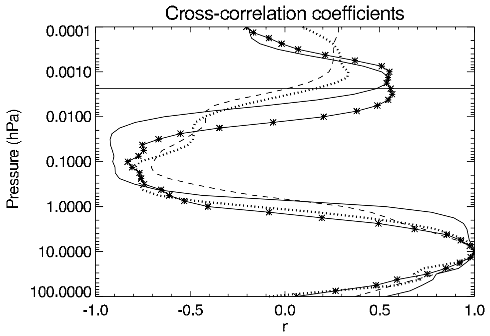

Figure 3. Cross correlation of detrended temperatures (see Figure 2) time series with reference at 10 hPa. Regions of positive correlation are interpreted as regions of stratospheric warming, regions of negative correlation are interpreted as regions of mesospheric cooling. The solid line is for Period 1 (80N), the short dashed line is Period 2 (80S) and the long dashed line is for Period 3 (80N), all calculated from zonal mean temperatures. The solid line with stars is from Period 2, at 70S and from a longitude sector from 40–100W, to roughly approximate the observation from Rothera shown in Figure 1. The horizontal line at.0024 hPa marks the approximate altitude of the OH* Meinel emission.

to 10^{-4} hPa with that at 10 hPa. The results for Periods 1–3 are shown in Figure 3. Figure 3 shows that stratospheric temperatures between 2–3 hPa and 50–70 hPa are highly correlated with the 10 hPa temperature. Moving above the stratopause, the temperature residuals become highly anticorrelated. We identify this as the mesospheric cooling regime which anticorrelates with the stratospheric warming regime. Note that at 0.3 hPa, we are well within the mesospheric cooling regime; thus, labeling this pressure as "stratospheric" as was done by *Cho et al.* [2004] appears to be inappropriate. Near 0.01 hPa, the strong anticorrelation rapidly disappears. Indeed, near 0.002 hPa, which is the pressure associated with the peak of the OH* emission, the correlation coefficient is close to zero or slightly positive. This means that temperature measurements from OH* emissions will likely not vary in concert with the underlying mesosphere. Also, this cross-over altitude, between negative and near zero r occurs much lower than predicted by *Liu and Roble* [2002]. Their results suggested a negative correlation extending up to ~110 km (see their Figure 3).

[12] At the highest altitudes the correlation coefficient becomes weakly positive. To assess the possible significance this value of r, we note that for 30–40 points, the 95% confidence interval is at $r = 0.30$ [*Bevington*, 1969] which is close to the values all three curves reach between $p = 10^{-3}$ and 10^{-4} hPa. This may suggest a region of positive correlation between the lower thermosphere and the stratosphere, analogous to the secondary thermospheric warming predicted by *Liu and Roble* [2002], albeit occurring at much lower altitudes than the 110–120 km they predicted.

[13] While the three zonal mean curves in Figure 3 show similar profile shapes, we recognize that ground-based OH* measurements are acquired for single locations and might be sampling regional temperatures that are not representative of the zonal mean. To address this possibility, a fourth curve in Figure 3 shows the cross-correlation for a 60° wide longitude and 10° wide latitude sector centered at 70W and 70S (the location of the Rothera OH* observations). This cross correlation profile is very similar to the three zonal mean residual curves. Our result is consistent with the analysis of *Sigernes et al.* [2003], who compared stratospheric temperatures in a 5° × 5° grid over Svalbard with OH* temperatures and found little anticorrelation over a 20 year period, (with one notable exception of the 1990–1991 winter).

[14] To get a better sense of the possible dynamics causing this upper mesospheric transition between negative and positive r, we present, in Figure 4, the geopotential height perturbations computed from SABER temperatures at 70S on Day 235 in Period 2. For this calculation, we used United Kingdom Meteorological Office 12Z geopotential height fields at 100 hPa as a bottom boundary. We then computed and subtracted the zonal mean geopotential height for each pressure level to get the perturbation amplitude. Figure 4 shows a well-defined wave 1 signature which extends up through the mesosphere to just above 0.1 hPa. The right hand panel shows a fit of a wave 1 sine wave to the perturbation geopotential. Above 0.1 hPa, the wave 1 amplitude is sharply attenuated, although there is a suggestion of a reamplification at the highest altitudes (100 km). While we should more properly show data using a formal asynoptic mapping procedure [e.g., *Remsberg et al.*, 2003], we have looked at data from other latitudes and adjacent days (234 and 236) and found these features to be quite stable in amplitude and phase. Thus we argue that biases from tidal aliasing can be neglected. We conclude that the decay of the wave 1 pattern above 0.1 hPa and the small enhancement near 100 km are real. Note that the altitude of the OH measurements (indicated by the white "R", for Rothera in Figure 4) occurs near an amplitude minimum. We thus suggest that the amplitude of the wave 1 and the correlation with stratospheric temperatures are linked; when the wave amplitude is a minimum (as it is at OH* altitudes), little correlation with stratospheric temperatures is seen.

[15] The possible reintensification above $p = 10^{-3}$ hPa may be related to the weak positive correlation seen at high

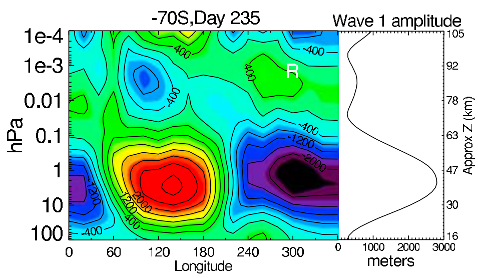

Figure 4. Plot of perturbation geopotential amplitude (meters) for Day 235, 2002, calculated by integrating the SABER temperatures at each longitude and subtracting the daily zonal mean (shown on the right hand axis) from each profile. The "R" in the upper right hand side of the plot represents the approximate pressure and longitude of the OH* Meinel measurements made at Rothera (68S,68W). The right hand panel shows the amplitude of the wave 1 obtained by linear regression to the color/contoured data.

altitudes in Figure 3. *Liu and Roble* [2002] suggest that altered gravity wave transmission into the lower thermosphere could drive a warming response. *Smith* [1996] also discusses the possibility of secondary planetary wave generation by zonally asymmetric gravity wave breaking in the mesosphere. In light of these suggestions, we suggest that the reamplified wave 1 seen in Figure 4 and the apparent correlation of the temperatures above 10^{-3} hPa with the 10 hPa temperature (i.e. thermospheric heating) may be related via vertical dynamical coupling.

4. Conclusion

[16] By cross-correlating SABER vertical temperature profiles with a reference point at 10 hPa, we can define a consistent behavior of the entire middle atmospheric temperature response. A stratospheric warming event will generally be vertically coherent from 50–100 hPa to 1 hPa. From about 0.3 hPa to 0.01 hPa, we find a strong anticorrelation with the underlying stratosphere, reproducing the classic mesospheric cooling response to SSWs [*Labitzke*, 1981]. Above 0.01 hPa, there are indications of another reversal in the temperature response with a weaker positive correlation with stratospheric temperatures. The lack of a clear correlation between stratospheric temperatures and the temperatures for $p < 0.01$ hPa suggests that OH Meinel Band temperatures ($p = 2 \times 10^{-3}$ hPa) may not be representative of the underlying mesospheric temperature response during SSWs, possibly explaining the equivocal findings of previous studies that have looked for such correlations observationally.

[17] While the existence of a clearly defined mesospheric cooling layer agrees with the calculations of *Liu and Roble* [2002], the observations clearly show that such a layer is much shallower in depth than the TIME-GCM predictions. Our observations do, however, agree with the general morphology shown by the hindcasting simulation for Period 2, described by *Coy et al.* [2005]. The possible weak positive correlations we suggest in the upper mesosphere may be consistent with the *Liu and Roble* [2002] suggestion of a net downwelling response to SSWs at high altitudes, possibly due to enhanced breaking of eastward traveling gravity waves. The increased wave 1 amplitude seen in the lower thermosphere by SABER on Day 235 of 2002 may also be consistent with TIME-GCM predictions of enhanced wave activity in the MLT. Certainly, the relative roles of gravity wave and planetary wave forcing in the MLT during these events need further elucidation.

[18] **Acknowledgments.** The TIMED satellite and the SABER instrument development and science analysis were all funded by the NASA Office of Space Science. In addition, we acknowledge support from the Office of Naval Research. We thank the SABER Instrument team for their hard work in data processing, Andrew Kochenash of Computatinal Physics Inc. for his assistance with the data analysis at NRL, and Steve Eckermann for helpful discussions.

References

Baldwin, M. P., and T. J. Dunkerton (2001), Stratospheric harbingers of anomalous weather regimes, *Science*, *294*, 581–584.

Bevington, P. R. (1969), *Data Reduction and Error Analysis for the Physical Sciences*, 336 pp., McGraw-Hill, New York.

Cho, Y.-M., G. G. Shepherd, Y.-I. Won, S. Sargoytchev, S. Brown, and B. Solheim (2004), MLT cooling during stratospheric warming events, *Geophys. Res. Lett.*, *31*, L10104, doi:10.1029/2004GL019552.

Coy, L., D. E. Siskind, S. D. Eckermann, J. P. McCormack, D. R. Allen, and T. F. Hogan (2005), Modeling the August 2002 minor warming event, *Geophys. Res. Lett.*, *32*, L07808, doi:10.1029/2005GL022400.

Emmert, J. T., J. M. Picone, J. L. Lean, and S. H. Knowles (2004), Global change in the thermosphere: Compelling evidence of a secular decrease in density, *J. Geophys. Res.*, *109*, A02301, doi:10.1029/2003JA010176.

Espy, P. J., R. E. Hibbins, G. O. L. Jones, D. M. Riggin, and D. C. Fritts (2003), Rapid, large-scale temperature changes in the polar mesosphere and their relationship to meridional flows, *Geophys. Res. Lett.*, *30*(5), 1240, doi:10.1029/2002GL016452.

Hernandez, G. (2003), Climatology of the upper mesosphere temperature above South Pole (90°S): Mesospheric cooling during 2002, *Geophys. Res. Lett.*, *30*(10), 1535, doi:10.1029/2003GL016887.

Hernandez, G. (2004), Winter mesospheric temperatures above South Pole (90°S) and their relationship to the springtime ozone hole size, *Geophys. Res. Lett.*, *31*, L07109, doi:10.1029/2004GL019414.

Labitzke, K. (1981), Stratospheric-mesospheric midwinter disturbances: A summary of characteristics, *J. Geophys. Res.*, *86*, 9665–9678.

Liu, H. L., and R. G. Roble (2002), A study of a self-generated stratospheric sudden warming and its mesospheric-lower thermospheric impacts using the coupled TIME-GCM/CCM3, *J. Geophys. Res.*, *107*(D23), 4695, doi:10.1029/2001JD001533.

McCormack, J. P., et al. (2004), NOGAPS-ALPHA model simulations of stratospheric ozone during the SOLVE-2 campaign, *Atmos. Chem. Phys.*, *4*, 2401–2423.

Mertens, C. J., et al. (2004), SABER observations of mesospheric temperatures and comparisons with falling sphere measurements taken during the 2002 summer MaCWAVE campaign, *Geophys. Res. Lett.*, *31*, L03105, doi:10.1029/2003GL018605.

Myrabo, H. K., C. S. Deehr, and R. Lybekk (1984), Polar cap OH airglow rotational temperatures at the mesopause during a stratospheric warming event, *Planet. Space Sci.*, *32*, 853.

Remsberg, E., G. Lingenfelser, V. L. Harvey, W. Grose, J. Russell III, M. Mlynczak, L. Gordley, and B. T. Marshall (2003), On the verification of the quality of SABER temperature, geopotential height, and wind fields by comparison with Met Office assimilated analyses, *J. Geophys. Res.*, *108*(D20), 4628, doi:10.1029/2003JD003720.

Roble, R. G., and R. E. Dickinson (1989), How will changes in carbon dioxide and methane modify the mean structure of the mesosphere and thermosphere, *Geophys. Res. Lett.*, *16*, 1441–1444.

Sigernes, F., N. Shumilov, C. S. Deehr, K. P. Nielsen, T. Svenøe, and O. Havnes (2003), Hydroxyl rotational temperature record from the auroral station in Adventdalen, Svalbard (78°N, 15°E), *J. Geophys. Res.*, *108*(A9), 1342, doi:10.1029/2001JA009023.

Smith, A. K. (1996), Longitudinal variations in mesospheric winds: Evidence for gravity wave filtering by planetary waves, *J. Atmos. Sci.*, *53*(8), 1156–1173.

L. Coy and D. E. Siskind, Naval Research Laboratory, Code 7640, 4555 Overlook Avenue SW, Washington, DC 20375, USA. (siskind@uap2.nrl.navy.mil)

P. Espy, Physical Sciences Division, British Antarctic Survey, Natural Environment Research Council, High Cross, Madingley Road, Cambridge CB3 0ET, UK.